Research Article

Cancer Immunology Research

Decitabine Enhances Lymphocyte Migration and Function and Synergizes with CTLA-4 Blockade in a Murine Ovarian Cancer Model

Lei Wang[1], Zohreh Amoozgar[1], Jing Huang[1], Mohammad H. Saleh[1], Deyin Xing[2], Sandra Orsulic[3], and Michael S. Goldberg[1]

Abstract

The lack of second-line treatment for relapsed ovarian cancer necessitates the development of improved combination therapies. Targeted therapy and immunotherapy each confer clinical benefit, albeit limited as monotherapies. Ovarian cancer is not particularly responsive to immune checkpoint blockade, so combination with a complementary therapy may be beneficial. Recent studies have revealed that a DNA methyl transferase inhibitor, azacytidine, alters expression of immunoregulatory genes in ovarian cancer. In this study, the antitumor effects of a related DNA methyl transferase inhibitor, decitabine (DAC), were demonstrated in a syngeneic murine ovarian cancer model. Low-dose DAC treatment increases the expression of chemokines that recruit NK cells and $CD8^+$ T cells, promotes their production of IFNγ and TNFα, and extends the survival of mice bearing subcutaneous or orthotopic tumors. While neither DAC nor immune checkpoint blockade confers durable responses as a monotherapy in this model, the efficacy of anti–CTLA-4 was potentiated by combination with DAC. This combination promotes differentiation of naïve T cells into effector T cells and prolongs cytotoxic lymphocyte responses as well as mouse survival. These results suggest that this combination therapy may be worthy of further consideration for improved treatment of drug-resistant ovarian cancer. *Cancer Immunol Res; 3(9); 1030–41. ©2015 AACR.*

Introduction

Effective treatment options for ovarian cancer remain limited, as most patients relapse. Immunotherapy can address disease that is refractory to conventional treatment options and represents an exciting new modality to achieve durable patient responses (1). Still, the percentage of such responders could be improved greatly. Improving the immunogenicity of tumors represents one approach to overcome a tumor's evasion of the immune system (2). Similarly, inhibiting immune checkpoint pathways, such as CTLA-4, which attenuates T-cell activation and related antitumor responses, can improve patient outcomes.

CTLA-4 blockade counteracts the immunosuppressive effects of regulatory T cells (Tregs; refs. 3, 4) and stimulates effector T-cell activation, expansion, function, and motility (5, 6). CTLA-4 blockade can also eliminate myeloid-derived suppressor cells (MDSC), which contributes to improving the survival of mice bearing ovarian tumors (7). The therapeutic benefits of targeting checkpoint blockade have been validated in patients with advanced solid tumors (8), including ovarian cancer (9). Although promising, the responses to date benefit only a minority of patients. The administration of an appropriate complementary therapy is expected to improve the magnitude and frequency of responses.

Epigenetic modifiers have gained considerable attention of late in the pursuit of antitumor compounds that do not impart the harsh side effects of cytotoxic chemotherapeutics, as epigenetic patterns differ between normal cells and cancer cells, enabling discrimination (10). The effects of these drugs are thought to be particularly profound in the context of cancer stem cells (11) and drug tolerance heterogeneity (12).

Although DNA hypomethylation is often thought to relieve repression of tumor suppressor genes (13), there is emerging evidence that DNA methyltransferase inhibitors induce expression of immunoregulatory genes in cancer cells (14, 15). Of the cancers investigated to date, this effect is most pronounced in ovarian cancer cells (16). Treatment of ovarian cancer cells with the DNA methyltransferase inhibitor DAC (17) results in expression of cancer–testis antigens and MHC class I, increasing cancer cell recognition by $CD8^+$ T cells (18). DAC similarly restores expression of cytokines, cancer–testis antigens, MHC class I and II, and costimulatory molecules in cancer patients (19, 20). These findings support the hypothesis that DAC will synergize with cancer immunotherapies.

In this study, we investigated the impact of DAC on global gene expression in ovarian cancer cells and found the most upregulated class to be immunoregulatory genes. We then confirmed that DAC

[1]Department of Cancer Immunology and AIDS, Dana-Farber Cancer Institute, Boston, Massachusetts. [2]Department of Pathology, Johns Hopkins University, Baltimore, Maryland. [3]Women's Cancer Program, Samuel Oschin Comprehensive Cancer Institute, Cedars-Sinai Medical Center, Los Angeles, California.

Note: Supplementary data for this article are available at Cancer Immunology Research Online (http://cancerimmunolres.aacrjournals.org/).

Current address for Z. Amoozgar: Department of Radiation Oncology, Massachusetts General Hospital, Boston, MA; and current address for J. Huang, Department of Immunology, School of Basic Medical Sciences, Peking University, Beijing, China.

Corresponding Author: Michael S. Goldberg, Dana-Farber Cancer Institute, 450 Brookline Avenue, Boston, MA 02215. Phone: 617-582-9840; Fax: 617-582-9610; E-mail: Michael_Goldberg1@dfci.harvard.edu

doi: 10.1158/2326-6066.CIR-15-0073

AACR

increases the infiltration and antitumor function of tumor-associated lymphocytes, which are associated with a survival benefit in subcutaneous (s.c.) and orthotopic ovarian tumors. Finally, we combined DAC with immune checkpoint blockade antibodies and found a synergy between DAC and CTLA-4. The mechanism of synergy is related to the kinetics of lymphocyte cytokine production, which is sustained by anti–CTLA-4 following early but transient induction by DAC. The combination of epigenetic modifiers and immune checkpoint blockade is currently being investigated in the treatment of non–small cell lung cancer (NCT01928576), and the data herein suggest that such a combination may benefit ovarian cancer patients as well.

Materials and Methods

Microarray analysis after DAC treatment

BR5FVB1-Akt cells, generated as previously described (21), were seeded in a 24-well plate overnight and were incubated with 10 mg/mL of DAC for 72 hours, changing the media and drug every 24 hours. Cells were harvested, and total RNA was extracted using the RNeasy Mini Kit (Qiagen). RNA concentration was measured using the Nanodrop (Thermo Fisher Scientific), and whole-transcript gene array (Mouse gene ST 2.0) was performed by the Molecular Biology Core Facility at Dana-Farber Cancer Institute (Boston, MA). The data were analyzed using Affymetrix Transcriptome Analysis Console software. A total of 34,472 genes were included in the analysis. A linear fold change of 2 was used as a minimum threshold value, and Gene Functional Classification Tool (DAVID Bioinformatics Resources 6.7, NIAID/NIH), Kyoto Encyclopedia of Genes and Genomes (KEGG) pathway analysis, and Gene Ontology map analysis were used to annotate pathways of differentially regulated genes. The data are deposited in the Gene Expression Omnibus (GEO) under the accession number GSE69454.

Quantitative reverse transcription PCR validation of gene expression changes upon DAC treatment

BR5FVB1-Akt cells were treated with DAC as above. The relative gene expression of *Ccl2*, *Ccl5*, *Cxcl10*, *Il6*, *Irf7*, and *Tnfrsf18* (*GitrL*) was measured using the Ambion Cells-to-CT Kit 1-Step Power SYBR Green Kit (Life Technologies) and the Applied Biosystems 7500 Fast Real-Time PCR System and Software. Mouse β-actin was used as the endogenous housekeeping gene for normalization. All quantitative reverse transcription PCR (qRT-PCR) assays were carried out in technical triplicate with biologic duplicate, and the experiments were repeated independently two to three times.

Mouse intraperitoneal and subcutaneous syngeneic ovarian cancer models

BR5FVB1-Akt cells were cultured in DMEM with 10% FBS and 1% penicillin/streptomycin at 37°C with 5% CO_2. Six-week-old female FVB mice were obtained from Charles River Laboratories. Mice were housed in a pathogen-free facility in accordance with the standards of the Dana-Farber Cancer Institute (Boston, MA). All animal experiments were approved by the Institutional Animal Care and Use Committee. Mice were kept in groups of 3 to 5 per cage in a 12-hour light/12-hour dark cycle and housed at 25°C with 50% relative humidity. For the intraperitoneal (i.p.) model, 4 million BR5FVB1-Akt cells were injected into the peritoneal cavity, and the mice were sacrificed upon development of pronounced ascites. In the absence of treatment, hemorrhagic ascites were formed 20 to 30 days after tumor cell inoculation. For the subcutaneous model, 2 million BR5FVB1-Akt cells were implanted s.c. into FVB mice on the left flank. Tumors formed 30 to 40 days after implantation, and the mice were sacrificed when the tumor size reached 2 cm^3.

Drug treatment and combination therapy *in vivo*

DAC was dissolved in DMSO (5 μL) and mixed with PBS (95 μL). One mg/kg of DAC (Selleckchem) was injected i.p. on days 4, 6, and 8 after BR5FVB1-Akt cell inoculation for both i.p. and s.c. models. For combinational therapy, 100 μg of anti–CTLA-4 antibody (clone: 9H10) or hamster IgG isotype control in PBS was additionally administered to mice on days 5, 7, and 9 after tumor inoculation. All antibodies were purchased from BioXCell. Mouse ascites and s.c. tumors were monitored daily.

Immunohistochemistry analyses of subcutaneous tumor sections

Tumors from solvent control- and DAC-treated groups were collected on day 42 and fixed in 4% paraformaldehyde at 4°C for at least 48 hours, followed by submerging the fixed tissues in 30% sucrose for 24 hours. The tissues were embedded in optimal cutting temperature (OCT) and cryosectioned to slices 10 μm in thickness. Slides were permeabilizied with 0.2% Triton in PBS and blocked in 2% BSA in PBS for 30 minutes prior to incubation with anti-mouse/rat FoxP3 antibody (eBiosciences 11-5773-82), anti-mouse CD8a antibody (Biolegend 100706), and anti-mouse CD45 antibody (Biolegend 103112) for 1 hour at room temperature. To enhance the green fluorescent signal, Alexa Fluor 488 Conjugate (Invitrogen A11096) was added after the primary antibody incubation. Slides were mounted in SlowFade Gold anti-fade reagent with 4′,6-diamidino-2-phenylindole (DAPI) and immediately imaged using a Leica TCS SP5 X confocal laser scanning microscope (Leica Microsystems Inc.).

Flow-cytometric analysis of tumor-infiltrating lymphocytes

Tumors were harvested on day 45 after tumor cell implantation, weighed dry, cut into small pieces, and incubated in collagenase solution in a 37°C water bath for 2 hours. GentleMACs was used at end of the incubation to improve homogenization. The dissociated tumors were passed through a 70-μm filter to generate single-cell suspensions, and red blood cells were lysed as necessary. Cells were blocked with 2% FBS and anti-mouse CD16/32 (TruStain fcX; Biolegend) in PBS for 10 minutes at 4°C. Next, they were stained with the following cocktail of fluorescently labeled antibodies: anti-CD3, anti-CD4, anti-CD8a, and anti-Nkp46. The cells were fixed and permeabilized using the FoxP3 buffer kit (eBioscience) for intracellular staining of FoxP3. Cells were then analyzed on a BD Fortessa or BD LSR II using FlowJo software.

Flow-cytometric analysis of tumor-associated lymphocytes in peritoneal cavity

The mice were sacrificed 14 or 42 days after tumor cell inoculation. A peritoneal wash was performed by injecting cold saline solution (2% FBS in PBS) into the mouse peritoneum, followed by gentle massage. The cell-containing saline solution was then collected. Again, red blood cells were lysed as necessary. For phenotypic analyses, the following antibodies were used: anti-CD3, anti-CD4, anti-CD8a, anti-CD44, anti-CD62L, anti-Ki67, anti-CD25, anti-Nkp46, anti-F4/80, anti-CD11b, anti-Gr1, anti-Ly6G, anti-CD11c, and anti-FoxP3. For functional assays, the cells were stimulated with phorbol 12-myristate

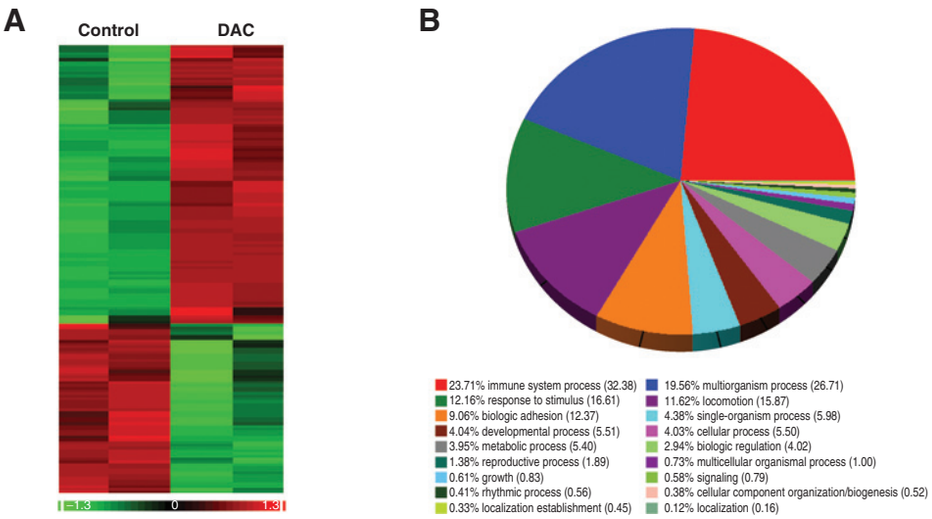

C

Upregulated gene sets KEGG pathway

Term	Genes
Cytokine–cytokine receptor interaction	*Cxcl1, Inhba, Ccl2, Pdgfb, Tnfrsf12a, Ccl5, Tnfsf18, Ccl7, Il1a, Cxcl10*
Chemokine signaling pathway	*Cxcl1, Ccl2, Ccl20, Ccl5, Ccl7, Cxcl10*
Cytosolic DNA-sensing pathway	*Ddx58, Irf7, Ccl5, Cxcl10*
NOD-like receptor signaling pathway	*Cxcl1, Ccl2, Ccl5, Ccl7*
RIG-I-like receptor signaling pathway	*Ddx58, Isg15, Irf7, Cxcl10*
MAPK signaling pathway	*Dusp4, Pdgfb, Flnb, Myc, Il1a*
Toll-like receptor signaling pathway	*Irf7, Ccl5, Cxcl10*

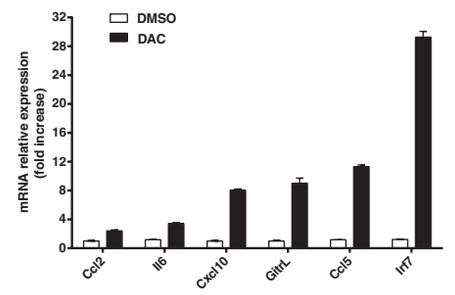

Figure 1.
DAC treatment activates expression of immunoregulatory genes. BR5FVB1-Akt ovarian cancer cells were treated with DAC for 72 hours, and total RNA was collected for mouse gene ST 2.0 microarray analysis. A, heatmap of DMSO control and DAC using unpaired one-way ANOVA ($P < 0.05$). Two independent biologic duplicates were evaluated, and the filter criterion was a linear fold change greater than 2. B, Gene Ontology (GO)-Map analysis reveals that immunoregulatory genes constitute the greatest percentage of upregulated genes by category. C, KEGG pathway analysis reveals that many of the upregulated gene sets are components of cytokine, chemokine, and innate immune signaling pathways. D, RT-PCR analysis confirms that treatment of BR5FVB1-Akt cells with DAC for 72 hours leads to upregulation of several immunoregulatory genes that can affect antitumor immunity.

13-acetate (PMA; 50 ng/mL) and ionomycin (500 ng/mL) with Golgi-Stop (BD Biosciences) in RPMI medium (supplemented with 10% FBS and 1% penicillin/streptomycin). An anti-CD107a antibody was also added during stimulation to evaluate degranulation. After stimulation, surface and intracellular staining were performed using the following antibodies: anti-CD3, anti-CD4, anti-CD8a, anti-Nkp46, anti-FoxP3, anti-IL10, anti-IFNγ, and anti-TNFα. Samples were analyzed on a BD Fortessa or BD LSR II using FlowJo software. All antibodies were purchased from Biolegend, except anti-Nkp46, which was purchased from eBioscience.

Statistical analysis

Statistical analyses were performed using a two-tailed Student *t* test (GraphPad Prism). Error bars denote mean ± SD. A *P* value of less than 0.05 was considered to be statistically significant (*, $P < 0.05$; **, $P < 0.005$; ***, $P < 0.0005$; ****, $P < 0.0001$).

Results

DAC treatment induces an immune-related gene expression signature

The DNA methyl transferase inhibitor azacitadine has immunomodulatory effects on multiple cancer types, particularly ovarian cancer (16). To explore the impact of the closely related DAC (17) on gene expression in this tumor model, we performed a genome-wide microarray analysis of BR5FVB1-Akt cells treated with DMSO control or DAC for 72 hours. Out of 34,472 unique genes investigated, 83 genes were upregulated and 28 genes were downregulated by at least 2-fold after DAC treatment. Heatmap analyses demonstrate that control- and DAC-treated cells exhibit different global gene expression profiles (Fig. 1A), and the most upregulated Gene Ontology signature is "immune system process" (Fig. 1B). KEGG pathway analysis reveals that the DAC upregulated genes are involved in multiple immune-related signaling pathways, such as cytokine–cytokine receptor interaction, chemokine signaling pathway, and MAPK and TLR signaling pathways (Fig. 1C). Their encoded proteins may contribute significantly to T-cell and NK-cell migration toward the tumor site and subsequent proliferation and antitumor function (22, 23).

The functional groups of the modulated genes were determined using Gene Functional Classification Tool (DAVID Bioinformatics Resources 6.7, NIAID/NIH) and are shown in Supplementary Table S1. To validate the microarray results, we assessed the levels of several noteworthy immune-related genes by quantitative PCR (qPCR). BR5FVB1-Akt cells were treated with DAC, and their RNA was harvested after 72 hours. qPCR analysis confirmed that treatment with DAC upregulates

all of the genes inspected (*Ccl2*, *Il6*, *Cxcl10*, *GitrL*, *Ccl5*, and *Irf7*; Fig. 1D). DAC treatment also upregulates surface major histocompatibility complex I (H-2Kq haplotype) on BR5FVB1-Akt cells in a dose-dependent manner (Supplementary Fig. S1). These results revealed an association between DAC treatment and the expression of immune-related genes.

DAC inhibits tumorigenicity *in vivo*

The therapeutic potential of DAC was subsequently examined *in vivo* using an orthotopic syngeneic tumor model. BR5FVB1-Akt cells were inoculated i.p. into FVB mice, and DAC was administered i.p. at a dose of 1.0 mg/kg on days 4, 6, and 8 after tumor inoculation (Fig. 2A). An equivalent volume (100 μL) of DMSO/PBS ("solvent") was administered to a second cohort as a negative control. The tumor-bearing mice developed hemorrhagic ascites gradually in the peritoneal cavity and had to be euthanized by day ~25 in the absence of treatment. Tumors were detectable postmortem as nodules of various sizes adherent to the omentum, peritoneal wall, or intestinal mesentery. The onset of ascites in DAC-treated mice was delayed by approximately 10 days, and the survival of these mice was significantly improved relative to control mice ($P < 0.01$, Fig. 2B).

DAC treatment enhances infiltration of NK cells and cytokine production by CD8$^+$ T and NK cells in the peritoneal cavity

Next, we sought to determine how DAC mediated its antitumor effect. Orthotopic tumors were generated, and tumor-bearing mice were treated with solvent or DAC as above. On day 14 after inoculation, peritoneal fluid was collected, and tumor-associated leukocytes (TAL) were analyzed by flow cytometry. Representative figures of flow-cytometric analysis for various leukocytes, such as CD4$^+$ helper T cells, CD8$^+$ cytotoxic T cells, NK cells, CD4$^+$ Tregs, and MDSCs, are shown (Fig. 3A). The percentage of NK cells increased and the percentage of MDSCs decreased in DAC-treated mice compared with those in control mice (Fig. 3A and B). The percentages of CD4$^+$ helper T cells, CD8$^+$ cytotoxic T cells, and Tregs did not differ significantly (Fig. 3B), nor did the percentages of macrophages, neutrophils, and dendritic cells (data not shown).

To elucidate the functional capacity of effector lymphocytes in the tumor environment, we evaluated the expression levels of IFNγ and TNFα among CD8$^+$ cytotoxic T lymphocytes and NK cells that had been recovered from control- or DAC-treated mice. Representative figures of flow-cytometric analysis of these immune effector molecules are shown for CD8$^+$ T cells and NK cells (Fig. 3C). After DAC treatment, the expression of both IFNγ and TNFα was significantly upregulated in both lymphocyte populations (Fig. 3D). These data suggest that DAC treatment recruits NK cells and promotes NK cell and CD8$^+$ T-cell antitumor function in the tumor microenvironment.

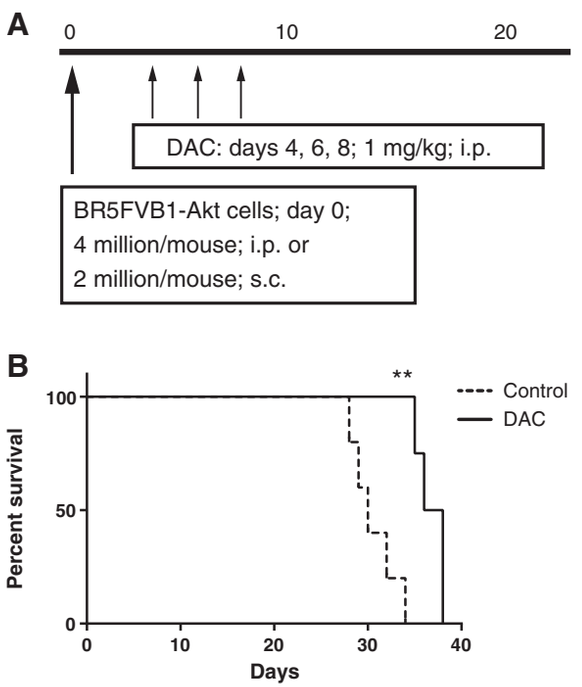

Figure 2.
DAC extends survival in a syngeneic orthotopic murine model of ovarian cancer. A, schematic of the dosing schedule used for *in vivo* drug treatment. BR5FVB1-Akt cells were i.p. injected into FVB mice, and DAC (1 mg/kg) was i.p. administered on days 4, 6, and 8 after tumor inoculation. B, Kaplan–Meier plot reveals that DAC extends the survival of FVB mice harboring syngeneic orthotopic ovarian tumors. At least 5 animals were used per group, and the experiment was performed independently three times. **, $P < 0.01$ versus control.

DAC treatment increases the number of intratumoral T cells and NK cells and recruits CD8$^+$ T cells into tumor-draining lymph nodes

As with the human presentation of the disease, the orthotopic tumor nodules are spread diffusely throughout the peritoneal cavity; therefore, harvesting sufficient bulk tissue is challenging for flow-cytometric analyses. Thus, to further investigate the phenotypes and functions of immune cells in solid tumor masses, s.c. tumors were generated. On day 45 after inoculation, tumors were collected, photographed, and weighed. Tumor-draining lymph nodes and spleens were also collected to enable a systematic study of the immune compartment. BR5FVB1-Akt cells were inoculated s.c. into FVB mice, and DAC was administered at a dose of 1.0 mg/kg via i.p. injection on days 4, 6, and 8 after tumor inoculation (Fig. 2A). An equivalent volume (100 μL) of solvent was administered to a second cohort as a negative control. More than one third of DAC-treated mice achieved a complete response (Fig. 4A), as evidenced by a lack of palpable tumor over 120 days. To inspect the mechanism underlying this survival benefit, additional cohorts of mice were sacrificed on day 35 after inoculation. Tumors isolated from mice receiving DAC exhibited a reduction in weight relative to tumors from control mice (Fig. 4B). The frequency of tumor-infiltrating CD8$^+$ cytotoxic T cells, NK cells, and CD4$^+$ helper T cells is increased in DAC-treated mice (Fig. 4C and E). A higher ratio of tumor-infiltrating CD8$^+$/Treg, which is associated with favorable prognosis in ovarian cancer (24), was also observed in DAC-treated mice.

We confirmed the increased density of CD8$^+$ T cells in tumor tissue by immunofluorescence staining and confocal imaging. Serial tumor biopsies from control and DAC-treated mice were stained for CD8, CD45, and DAPI. We found very few infiltrating CD8$^+$ T cells or CD45$^+$ leukocytes in tumors from control mice but a reasonably dense infiltrate of these cells in tumors from DAC-treated mice (Fig. 4G and Supplementary Fig. S2), mirroring the flow cytometry findings for CD8$^+$ T cells. CD8$^+$ T cells were also observed in elevated concentrations in tumor-draining lymph nodes following treatment (Fig. 4D and F). In contrast,

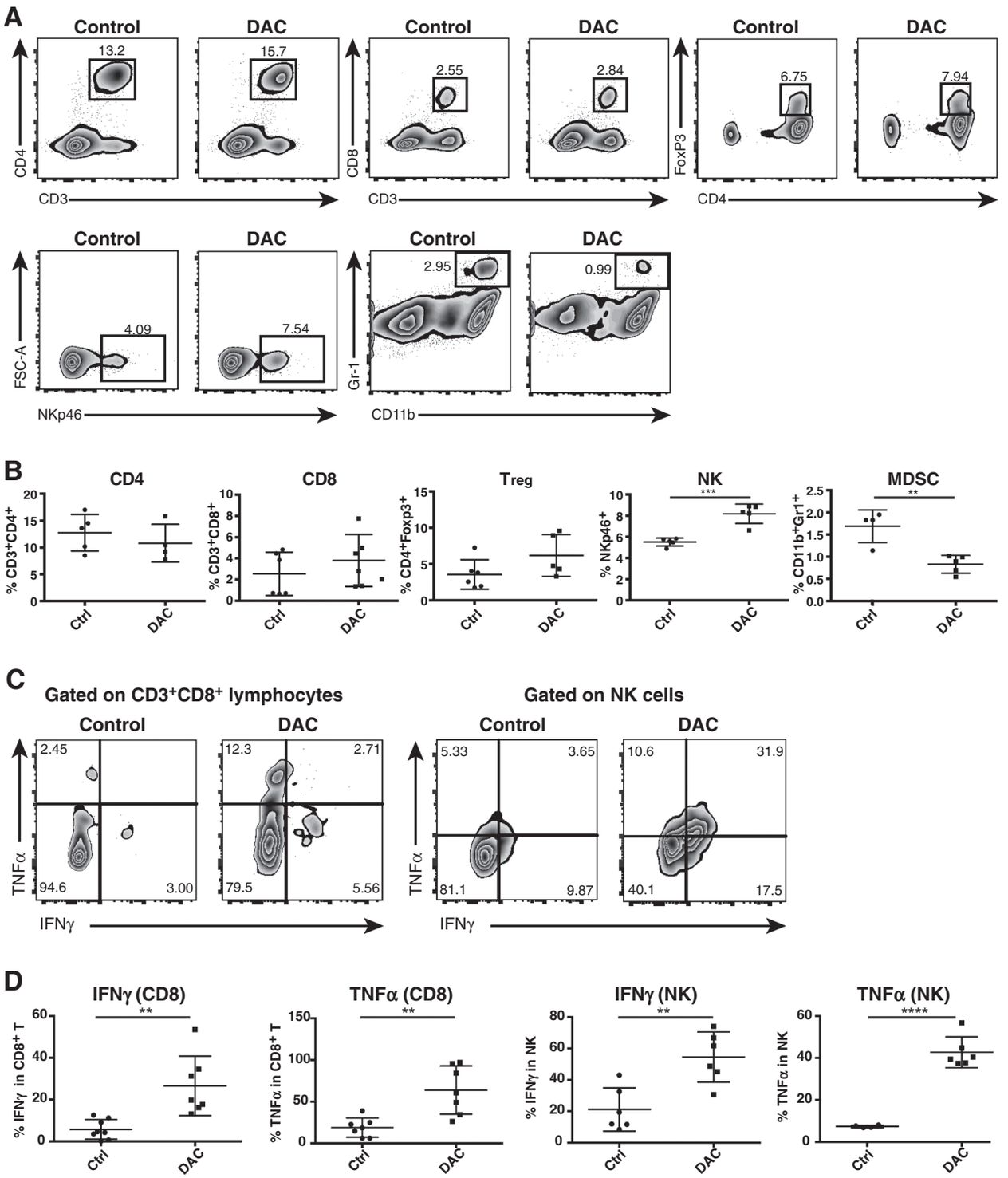

Figure 3.

DAC treatment alters immune cell composition and enhances cytokine production in the peritoneal lavage. FVB mice were dosed according to the schema in Fig. 2A. On day 14 after tumor inoculation, a peritoneal wash was performed, and single-cell suspensions were analyzed by flow cytometry. A, representative figures of flow-cytometric analyses of tumor-associated $CD4^+$ T cells, $CD8^+$ T cells, $CD4^+Foxp3^+$ Tregs, NK cells, and $CD11b^+Gr1^+$ MDSCs among control- and DAC-treated mice. B, quantitation of results from A with statistical analysis. C and D, cell suspensions from the peritoneal wash were stimulated with PMA and ionomycin for 4 hours, and stimulated cells were then analyzed for expression of CD3, CD8, Nkp46, IFNγ, and TNFα by flow cytometry. C, representative results are shown for control- and DAC-treated cells. D, quantitation of results from C with statistical analysis. **, $P < 0.005$; ***, $P < 0.0005$; ****, $P < 0.0001$. Representative of three independent experiments.

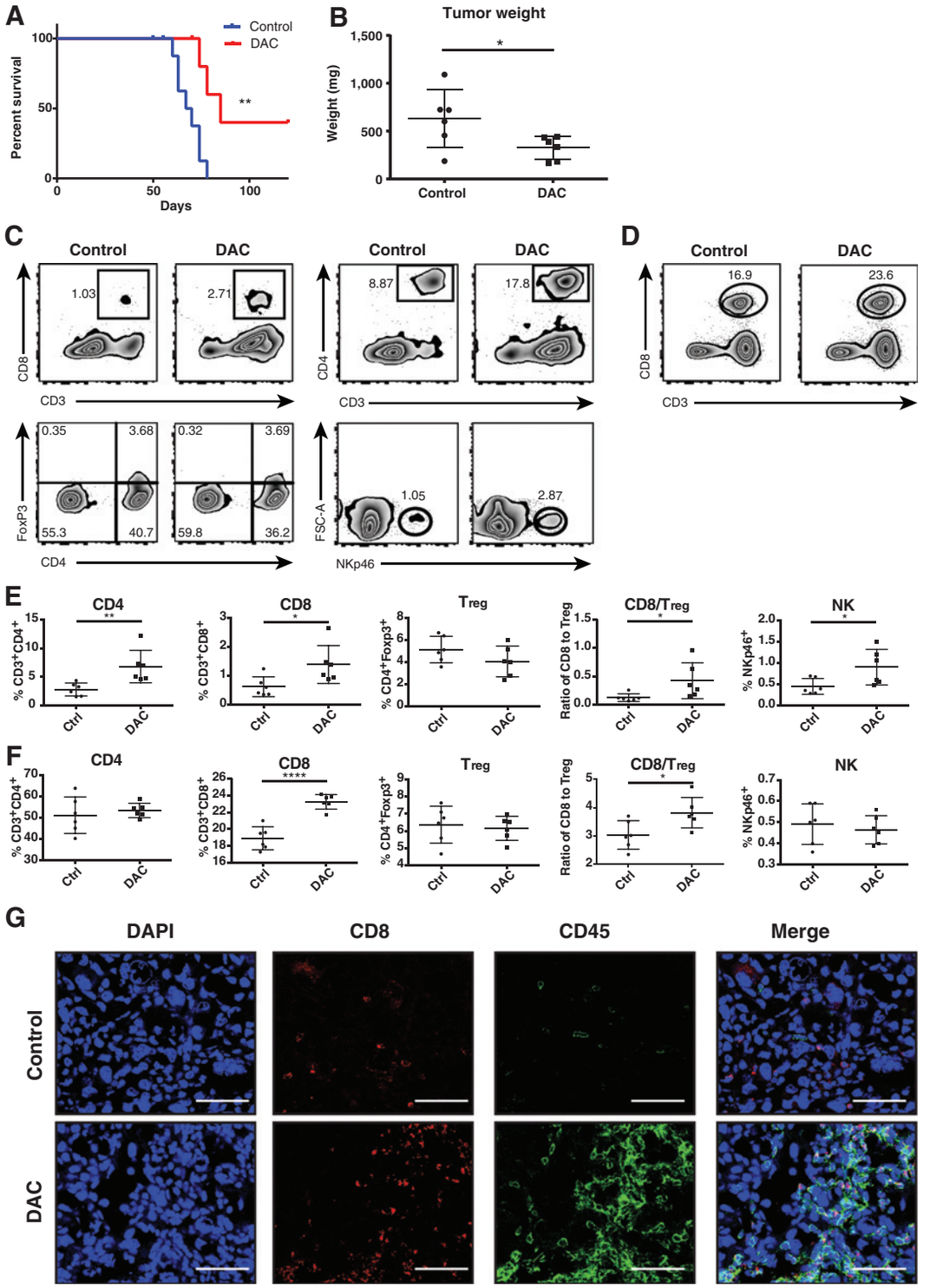

Figure 4.
Decitabine increases the frequency of tumor-infiltrating lymphocytes in s.c. tumors and tumor-draining lymph nodes. Tumor cells were implanted s.c. into FVB mice, which were dosed according to the schema in Fig. 2A. A, Kaplan–Meier plot reveals the survival benefit of DAC in the context of s.c. tumor inoculation. B–G, mice were sacrificed on day 35 after tumor inoculation, and tumors and tumor-draining lymph nodes were isolated. B, tumor weight of s.c. tumors confirms the benefit of DAC treatment. C, representative figures of flow-cytometric analyses of tumor-infiltrating $CD4^+$ T cells, $CD8^+$ T cells, $CD4^+Foxp3^+$ Tregs, and NK cells among control- and DAC-treated mice. D, representative figures of flow-cytometric analyses of $CD8^+$ T cells and $CD4^+Foxp3^+$ Tregs in tumor-draining lymph nodes among control- and DAC-treated mice. E, quantitation of results from C with statistical analysis. F, quantitation of results from D with statistical analysis. G, CD8 and CD45 expression were analyzed by immunofluorescence of s.c. tumors isolated from mice treated with solvent control or DAC. Scale bar, 50 μm. Representative sections are shown.

their numbers in the spleen were unaltered by DAC treatment (data not shown), indicating that the drug's effects are concentrated at the s.c. tumor site and tumor-draining lymph node despite being administered i.p.

CTLA-4 blockade synergizes with DAC to extend the survival of tumor-bearing mice

DAC exhibited significant but incomplete therapeutic efficacy as a monotherapy in this ovarian cancer model. This mechanistic study reveals that DAC modulates the function of $CD8^+$ T cells and NK cells in the peritoneum and increases their frequency in s.c. tumors. We hypothesized that immune checkpoint blockade would synergize with DAC therapy to combat tumorigenicity and promote antitumor immunity by enhancing $CD8^+$ T-cell and NK cell responses. Orthotopic tumors were generated, and tumor-bearing mice were dosed according to the schedule in Fig. 5A. Combining DAC with anti–CTLA-4 substantially delayed the onset of ascites relative to either monotherapy, with a majority of the mice achieving a complete response for a period of 90 days after tumor inoculation (Fig. 5B).

Combination treatment increases effector memory T-cell density, inflammatory cytokine production, and degranulation

Next, we inspected the mechanism underlying the survival benefit achieved by combining DAC and anti–CTLA-4. Orthotopic tumors were generated, and tumor-bearing mice were administrated with either DAC plus isotype antibody or DAC plus CTLA-4 blockade, following the same dosing schedule shown in Fig. 5A. On day 42 after tumor inoculation, peritoneal fluid was collected and TALs were analyzed. Phenotype analysis of $CD8^+$ T cells, $CD4^+$ T cells, Tregs, and NK cells showed no significant changes between two groups (data not shown). However, effector memory ($CD44^{hi}CD62L^{lo}$) $CD8^+$ and $CD4^+$ T-cell populations were highly enriched, with a concomitant decrease in naïve T cells in the combination group relative to DAC monotherapy (Fig. 6A–D). Ki67 expression on TALs was also increased in both $CD8^+$ and $CD4^+$ T-cell populations (Fig. 6E and F), indicating increased cell proliferation. The frequency of central memory T cells was unaffected by CTLA-4 blockade (Fig. 6A–D).

Production of IFNγ and TNFα by $CD8^+$ T cells (Fig. 6G and H) and NK cells (Fig. 6I and J) was elevated in the combination group, suggesting that these cells were functionally engaged in antitumor immunity. Indeed, NK cells exhibited increased degranulation, as determined by CD107a staining (Fig. 6K and L), suggesting that NK cells directly execute cell killing in the context of the increased proinflammatory microenvironment. Notably, CTLA-4 was recently shown to be expressed on NK cells upon their activation and to inhibit their production of IFNγ (25). Consistently, we observed that CTLA-4 blockade promotes IFNγ production by NK cells.

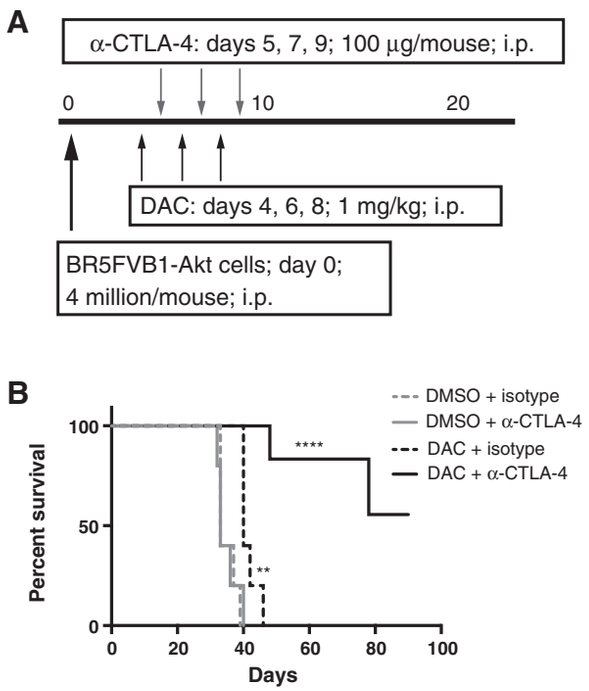

Figure 5.
Anti–CTLA-4 (α–CTLA-4) synergizes with DAC to extend the survival of mice harboring syngeneic orthotopic ovarian tumors. A, dosing schedule of DAC and immune checkpoint blockade. BR5FVB1-Akt cells were injected i.p. into FVB mice, and DAC (1 mg/kg) was administered on days 4, 6, and 8 after tumor inoculation. One hundred micrograms of anti–CTLA-4 or isotype antibody was injected on days 5, 7, and 9. All drugs were administered via i.p. injection. B, Kaplan–Meier plot reveals, unlike either monotherapy, the combination of DAC + anti–CTLA-4 dramatically improves survival. The experiment was concluded at day 90, which is twice the lifespan of mice treated with DAC monotherapy. At least 5 animals were used per group, and the experiment was performed independently three times. ****, $P < 0.0001$.

Immune response to DAC is sustained by the addition of anti–CTLA-4

TALs in DAC-treated mice displayed high cytokine production at an early time point (day 14) relative to the control group (Fig. 4A) but relatively low cytokine secretion at a late time point (day 42; Fig. 7A). We therefore investigated TAL function of the DAC plus isotype group and the DAC plus anti–CTLA-4 group at early and late stages of the disease. As described above, peritoneal fluid from mice treated with DAC plus isotype or DAC plus anti–CTLA-4 was collected. Cytokine production from $CD8^+$ T and NK cells was analyzed on days 14 and 42 after tumor inoculation. We surprisingly observed a slight decrease of lymphocyte function after the addition of anti–CTLA-4 at the early time point (Fig. 7; $P > 0.05$ in Fig. 7A–C and $P = 0.0129$ in Fig. 7D). However, lymphocyte function was greatly decreased at day 42, compared with day 14, in the DAC plus isotype group. In contrast, relatively high levels of cytokine were sustained in the combination treatment group at the later time point (Fig. 7). These data suggest that the immune response initiated in response to DAC treatment can be prolonged by the addition of anti–CTLA-4.

Discussion

In this study, we evaluated a novel drug combination regimen for epithelial ovarian cancer and explored the underlying mechanisms using an orthotopic mouse model. The approach uses an epigenetic modifier, DAC, in combination with immune checkpoint blockade, anti–CTLA-4. We show a prolonged cytotoxic lymphocyte response in the context of combination therapy and the resultant synergetic effect on survival.

From animal experiments to clinical trials, DAC has been investigated as a sensitizer to immunotherapy (26). Of note, its ability to induce expression of cancer–testis antigens (19, 27), most notably NY-ESO-1, for improved vaccination of ovarian cancer patients (28), is well established. Microarray analysis

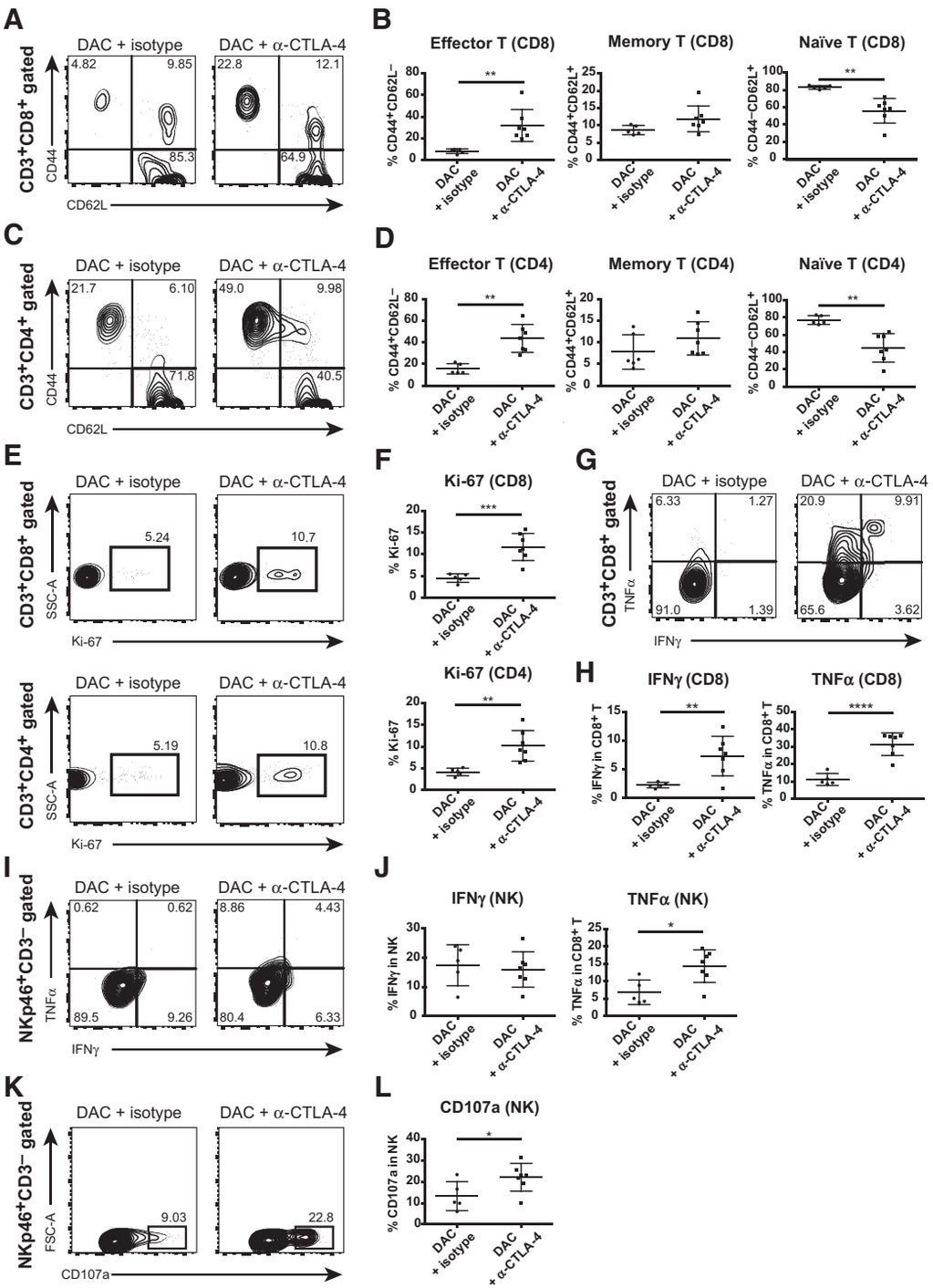

Figure 6.

Combining DAC with anti–CTLA-4 (α-CTLA-4) promotes the development of effector T cells in the peritoneal cavities of tumor-bearing mice. The FVB mice were divided into two treatment groups (DAC + isotype control and DAC + anti–CTLA-4), and cells isolated from their peritoneal cavities were analyzed on day 42 after tumor cell inoculation. A, representative flow cytometry plots for effector, memory, and naïve $CD8^+$ T cells. B, quantitation of results from A with statistical analysis. C, representative flow cytometry plots for effector, memory, and naïve $CD4^+$ T cells. D, quantitation of results from C with statistical analysis. E, representative flow cytometry plots for Ki-67 (cell proliferation marker) in $CD8^+$ and $CD4^+$ T cells. F, quantitation of results from E with statistical analysis. G–L, cell suspensions from the peritoneal wash were stimulated with PMA and ionomycin for 4 hours. Anti–CD107a was added during stimulation. The stimulated cells were analyzed for expression of CD3, CD8, Nkp46, CD107a, IFNγ, and TNFα by flow cytometry. G, representative flow cytometry plots for IFNγ and TNFα production in $CD8^+$ T cells. H, quantitation of results from G with statistical analysis. I, representative flow cytometry plots for IFNγ and TNFα production in NK cells. J, quantitation of results from I with statistical analysis. K, representative flow cytometry plots for CD107a expression in NK cells. L, quantitation of results from K with statistical analysis.

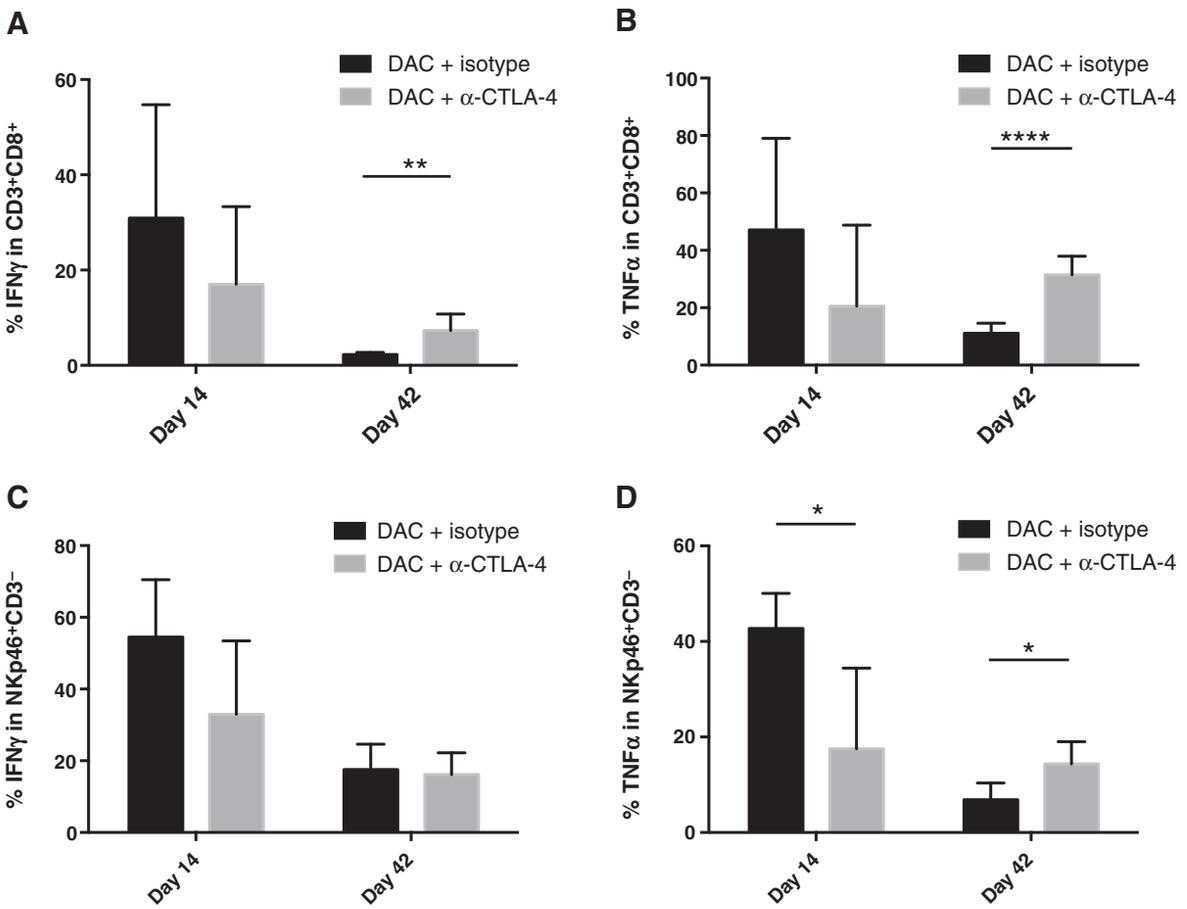

Figure 7.
Kinetics of IFNγ and TNFα production by $CD8^+$ T cells and NK cells during disease progression. The FVB mice were divided into two treatment groups [DAC + isotype control and DAC + anti–CTLA-4 (α-CTLA-4)] and cells isolated from their peritoneal cavities were analyzed on days 14 and 42 after tumor cell inoculation. Cell suspensions from the peritoneal wash were stimulated with PMA and ionomycin for 4 hours. α-CD107a was added during stimulation. The stimulated cells were analyzed for expression of CD3, CD8, Nkp46, IFNγ, and TNFα by flow cytometry. A, IFNγ production in $CD8^+$ T cells. B, TNFα production in $CD8^+$ T cells. C, IFNγ production in NK cells. D, TNFα production in NK cells.

previously demonstrated that azacitadine, another clinically available hypomethylating agent, yields substantial immunomodulatory effects on ovarian cancer cell lines (16). Our microarray data are in agreement with those from the previous report and show that the most upregulated Gene Ontology signature is "immune system process" after 3 days of DAC treatment. The upregulated genes are involved in several significant pathways that regulate T-cell trafficking and function. For example, the chemokines CCL2, CCL5, and CXCL10 are known to contribute to NK-cell (29, 30) and $CD8^+$ T-cell (31, 32) recruitment into the tumor microenvironment. Upregulation of these genes is expected to promote lymphocyte infiltration and antitumor function. Although cellular stress is likely partially responsible for the observed effects, DAC is not particularly cytotoxic at the dosage used (Supplementary Fig. S3), supporting the notion that epigenetic modification is important to the phenotype (14–16).

DAC treatment additionally increases expression of *Tnfsf18* (*GitrL*), which is the ligand for the T-cell costimulatory molecule GITR. GITR ligation enhances the infiltration and activity of effector T cells (33) and NK cells (22, 34) and generates effector T cells that are resistant to the immunosuppressive effects of Tregs (35). These data suggest that DAC not only has cancer cell–intrinsic antitumor effects but also modifies the tumor microenvironment to promote T-cell infiltration and antitumor function. DAC does not affect T-cell proliferation *in vitro* (data not shown), suggesting that DAC's effect on T cells is indirect, mediated through the drug's action on cancer cells. DAC also directly augments NK-cell responses to activating stimuli, such as IL2 or target cancer cells, and promotes NK cell–mediated cytotoxicity and IFNγ production *in vitro* by inducing transcription of genes involved in NK reactivity (36). These effects contrast with the impact of the related compound azacytidine, which impairs NK function (36).

We then evaluated the therapeutic benefits of DAC in an orthotopic ovarian cancer model using the BR5FVB1-Akt cell line, which lacks *p53* and *Brca1* and overexpresses *Myc* and *Akt*. These genetic alterations recapitulate the most common genetic alterations observed among ovarian cancer patients (37, 38). Importantly, this animal model resembles the human disease phenotypically as well as genetically. As seen in the human presentation

of ovarian cancer, the cancer cells disseminate throughout the peritoneal cavity and metastasize to the peritoneum wall, intestine, liver, and spleen, causing hemorrhagic ascites as well as occasional bowel obstruction and cachexia. Treating mice with DAC significantly delays ascites formation as well as tumor growth. Subcutaneous tumors in mice that received DAC exhibit a significant reduction in growth, with 40% of these mice achieving a complete response.

Immune cell phenotyping shows that DAC-treated mice recruit more NK cells and fewer MDSCs into their peritoneal cavities. MDSCs promote tumor progression via multiple suppressive mechanisms (39). Consistent with our results, it has been observed that the frequency of tumor-infiltrating MDSCs is also decreased in the B16 murine melanoma model in response to DAC treatment (40). NK cells are important in innate immune responses against tumors by direct cytolysis of cancer cells (41) and by antibody-dependent cellular cytotoxicity (ADCC; ref. 42). The low response rate associated with trastuzumab (anti-HER2) monotherapy is thought to be related to impaired NK-cell function in patients with advanced disease, suggesting that treatments that improve NK-cell activity may promote ADCC in addition to direct cytolysis (43). Thus, DAC might be particularly useful in combination with a depleting isotype of anti–PD-L1, promoting infiltration of NK cells while augmenting their ability to kill PD-L1–expressing epithelial cancer cells and MDSCs.

In the orthotopic setting, DAC enhances the function of tumor-associated $CD8^+$ T cells and NK cells. Production of the Th1 cytokines IFNγ and TNFα is greatly increased in $CD8^+$ T and NK cells isolated from DAC-treated mice. These proinflammatory cytokines play a critical role in surveillance against ovarian tumor development (44). In addition, DAC treatment induces CD80 expression on cancer cells and stimulates tumor-specific cytotoxic T- lymphocyte responses (45). Consistently, CD80 expression on BR5FVB1-Akt cells is increased 3-fold following DAC treatment *in vitro* (Supplementary Fig. S3). CD80 may be further upregulated *in vivo* owing to the increased IFNγ and TNFα production from TILs, as surface expression of CD80 can be induced in cancer cell lines and fibroblasts in response to IFNγ and TNFα stimulation (46, 47).

CTLA-4 is a homolog of the costimulatory molecule CD28 and acts to suppress T-cell function by competing with CD28 for their shared ligands CD80 and CD86 on antigen-presenting cells and many cancer cells. Binding of CTLA-4 to these ligands inhibits TCR signaling. Anti–CTLA-4 can reverse such immunosuppression by limiting the activity of tumor-infiltrating Tregs and through FcγR-dependent depletion of intratumoral Tregs (4). CTLA-4 expression is induced on $CD4^+$ and $CD8^+$ T cells following activation and is constitutively expressed on Tregs (48). A recent study demonstrated that CTLA-4 is also expressed on NK cells upon activation and inhibits their production of IFNγ (25). Together, these findings support the potential synergy between DAC and anti–CTLA-4.

This therapeutic combination yields a much greater antitumor effect than either treatment alone. Mechanistically, the combination promotes the differentiation of naïve T cells into effector $CD8^+$ and $CD4^+$ T cells and enhances their proliferation in the peritoneal cavity. Tumor-associated $CD8^+$ T cells and NK cells also express more IFNγ and TNFα upon addition of the CTLA-4–blocking antibody. A kinetic analysis comparing early- and late-stage disease (14 days vs. 42 days after tumor cell inoculation) reveals that the immune response to DAC is early and transient, but it can be sustained by the addition of anti–CTLA-4. Specifically, the cytotoxic lymphocytes produce high levels of IFNγ and TNFα at day 14, with slightly higher cytokine production in DAC monotherapy than in the combination therapy at this early time point. In contrast, at the later time point, addition of anti–CTLA-4 substantially augments cytokine production, prolonging the benefits of DAC treatment. Recent literature suggests that anti–CTLA-4 enhances $CD8^+$ T-cell effector memory formation, function, and maintenance (49), which is consistent with our findings. Of note, the combination also enhances NK cell degranulation, which is a surrogate for direct cancer cell killing. The importance of NK cell and T-cell crosstalk in the tumor microenvironment has been described recently (45). Specifically, the infiltration of both NK cells and $CD8^+$ T cells into colorectal cancer is associated with prolonged patient survival.

In summary, the combination therapy achieves its antitumor efficacy by stimulating both innate and adaptive immunity, influencing lymphocyte infiltration, differentiation, cytokine production, and cytolysis. The results provide a rationale for the clinical translation of a regimen combining epigenetic modifiers and immune checkpoint blockade and suggest that this combination may extend the survival of ovarian cancer patients.

Disclosure of Potential Conflicts of Interest

No potential conflicts of interest were disclosed.

Authors' Contributions

Conception and design: L. Wang, Z. Amoozgar, J. Huang, M.S. Goldberg
Development of methodology: L. Wang, Z. Amoozgar, J. Huang
Acquisition of data (provided animals, acquired and managed patients, provided facilities, etc.): L. Wang, Z. Amoozgar, J. Huang, M.H. Saleh, S. Orsulic
Analysis and interpretation of data (e.g., statistical analysis, biostatistics, computational analysis): L. Wang, Z. Amoozgar, M.H. Saleh
Writing, review, and/or revision of the manuscript: L. Wang, Z. Amoozgar, J. Huang, M.H. Saleh, S. Orsulic, M.S. Goldberg
Administrative, technical, or material support (i.e., reporting or organizing data, constructing databases): L. Wang, M.H. Saleh, D. Xing
Study supervision: L. Wang, M.S. Goldberg

Acknowledgments

The authors thank Lina Wu (Peking University Cancer Hospital and Institute) for microarray data analysis and Hye-Jung Kim and Jianmei Leavenworth for helpful discussions.

Grant Support

This work was supported by the Ovarian Cancer Research Fund (Liz Tilberis Scholar), Aid for Cancer Research, Kaleidoscope of Hope, and the Susan F. Smith Center for Women's Cancer.

The costs of publication of this article were defrayed in part by the payment of page charges. This article must therefore be hereby marked *advertisement* in accordance with 18 U.S.C. Section 1734 solely to indicate this fact.

Received March 16, 2015; revised May 7, 2015; accepted May 26, 2015; published OnlineFirst June 8, 2015.

References

1. Mellman I, Coukos G, Dranoff G. Cancer immunotherapy comes of age. Nature 2011;480:480–9.
2. Hanahan D, Weinberg RA. Hallmarks of cancer: the next generation. Cell 2011;144:646–74.

3. Nishikawa H, Sakaguchi S. Regulatory T cells in cancer immunotherapy. Curr Opin Immunol 2014;27:1–7.
4. Simpson TR, Li F, Montalvo-Ortiz W, Sepulveda MA, Bergerhoff K, Arce F, et al. Fc-dependent depletion of tumor-infiltrating regulatory T cells co-defines the efficacy of anti-CTLA-4 therapy against melanoma. J Exp Med 2013;210:1695–710.
5. Eagar TN, Turley DM, Padilla J, Karandikar NJ, Tan L, Bluestone JA, et al. CTLA-4 regulates expansion and differentiation of Th1 cells following induction of peripheral T cell tolerance. J Immunol 2004; 172:7442–50.
6. Pentcheva-Hoang T, Simpson TR, Montalvo-Ortiz W, Allison JP. Cytotoxic T lymphocyte antigen-4 blockade enhances antitumor immunity by stimulating melanoma-specific T-cell motility. Cancer Immunol Res 2014; 2:970–80.
7. Liu Y, Yu Y, Yang S, Zeng B, Zhang Z, Jiao G, et al. Regulation of arginase I activity and expression by both PD-1 and CTLA-4 on the myeloid-derived suppressor cells. Cancer Immunol Immunother 2009; 58:687–97.
8. Postow MA, Callahan MK, Wolchok JD. Immune checkpoint blockade in cancer therapy. J Clin Oncol 2015;33:1974–82.
9. Brahmer JR, Tykodi SS, Chow LQ, Hwu W-JJ, Topalian SL, Hwu P, et al. Safety and activity of anti-PD-L1 antibody in patients with advanced cancer. N Engl J Med 2012;366:2455–65.
10. Rodríguez-Paredes M, Esteller M. Cancer epigenetics reaches mainstream oncology. Nat Med 2011;17:330–9.
11. Jones PA, Baylin SB. The epigenomics of cancer. Cell 2007;128:683–92.
12. Sharma SV, Lee DY, Li B, Quinlan MP, Takahashi F, Maheswaran S, et al. A chromatin-mediated reversible drug-tolerant state in cancer cell subpopulations. Cell 2010;141:69–80.
13. Paz MF, Fraga MF, Avila S, Guo M, Pollan M, Herman JG, et al. A systematic profile of DNA methylation in human cancer cell lines. Cancer Res 2003;63:1114–21.
14. Tsai H, Li H, Van Neste L, Cai Y, Robert C, Rassool FV, et al. Transient low doses of DNA-demethylating agents exert durable antitumor effects on hematological and epithelial tumor cells. Cancer Cell 2012;21: 430–46.
15. Wrangle J, Wang W, Koch A, Easwaran H, Mohammad HP, Vendetti F, et al. Alterations of immune response of non-small cell lung cancer with azacytidine. Oncotarget 2013;4:2067–79.
16. Li H, Chiappinelli KB, Guzzetta AA, Easwaran H, Yen R-WCW, Vatapalli R, et al. Immune regulation by low doses of the DNA methyltransferase inhibitor 5-azacitidine in common human epithelial cancers. Oncotarget 2014;5:587–98.
17. Sabado RL, Pavlick A, Gnjatic S, Cruz CM, Vengco I, Hasan F, et al. Resiquimod as an immunologic adjuvant for NY-ESO-1 protein vaccination in patients with high-risk melanoma. Cancer Immunol Res 2015; 3:278–87.
18. Adair SJ, Hogan KT. Treatment of ovarian cancer cell lines with 5-aza-2′-deoxycytidine upregulates the expression of cancer-testis antigens and class I major histocompatibility complex encoded molecules. Cancer Immunol Immunother 2009;58:589–601.
19. Dubovsky JA, McNeel DG, Powers JJ, Gordon J, Sotomayor EM, Pinilla-Ibarz JA. Treatment of chronic lymphocytic leukemia with a hypomethylating agent induces expression of NXF2, an immunogenic cancer testis antigen. Clin Cancer Res 2009;15:3406–15.
20. Woloszynska-Read A, Mhawech-Fauceglia P, Yu J, Odunsi K, Karpf AR. Intertumor and intratumor NY-ESO-1 expression heterogeneity is associated with promoter-specific and global DNA methylation status in ovarian cancer. Clin Cancer Res 2008;14:3283–90.
21. Xing D, Orsulic S. A mouse model for the molecular characterization of brca1-associated ovarian carcinoma. Cancer Res 2006;66: 8949–53.
22. Placke T, Kopp H-GG, Salih HR. Glucocorticoid-induced TNFR-related (GITR) protein and its ligand in antitumor immunity: functional role and therapeutic modulation. Clin Dev Immunol 2010;2010:239083.
23. Koizumi K, Hojo S, Akashi T, Yasumoto K, Saiki I. Chemokine receptors in cancer metastasis and cancer cell-derived chemokines in host immune response. Cancer Sci 2007;98:1652–8.
24. Sato E, Olson SH, Ahn J, Bundy B, Nishikawa H, Qian F, et al. Intraepithelial CD8+ tumor-infiltrating lymphocytes and a high CD8+/regulatory T cell ratio are associated with favorable prognosis in ovarian cancer. Proc Natl Acad Sci U S A 2005;102:18538–43.
25. Stojanovic A, Fiegler N, Brunner-Weinzierl M, Cerwenka A. CTLA-4 is expressed by activated mouse NK cells and inhibits NK cell IFN-γ production in response to mature dendritic cells. J Immunol 2014; 192:4184–91.
26. Li X, Mei Q, Nie J, Fu X, Han W. Decitabine: a promising epi-immunotherapeutic agent in solid tumors. Expert Rev Clin Immunol 2015;11: 363–75.
27. Cruz CR, Gerdemann U, Leen AM, Shafer JA, Ku S, Tzou B, et al. Improving T-cell therapy for relapsed EBV-negative Hodgkin lymphoma by targeting upregulated MAGE-A4. Clin Cancer Res 2011; 17:7058–66.
28. Odunsi K, Matsuzaki J, James SR, Mhawech-Fauceglia P, Tsuji T, Miller A, et al. Epigenetic potentiation of NY-ESO-1 vaccine therapy in human ovarian cancer. Cancer Immunol Res 2014;2:37–49.
29. Ottaviani C, Nasorri F, Bedini C, de Pità O, Girolomoni G, Cavani A. CD56brightCD16(−) NK cells accumulate in psoriatic skin in response to CXCL10 and CCL5 and exacerbate skin inflammation. Eur J Immunol 2006;36:118–28.
30. Muenchmeier N, Boecker S, Bankel L, Hinz L, Rieth N, Lapa C, et al. A novel CXCL10-based GPI-anchored fusion protein as adjuvant in NK-based tumor therapy. PLoS ONE 2013;8:e72749.
31. Harlin H, Meng Y, Peterson AC, Zha Y, Tretiakova M, Slingluff C, et al. Chemokine expression in melanoma metastases associated with CD8+ T-cell recruitment. Cancer Res 2009;69:3077–85.
32. Kunz M, Toksoy A, Goebeler M, Engelhardt E, Bröcker E, Gillitzer R. Strong expression of the lymphoattractant C-X-C chemokine Mig is associated with heavy infiltration of T cells in human malignant melanoma. J Pathol 1999;189:552–8.
33. Burckhart T, Thiel M, Nishikawa H, Wüest T, Müller D, Zippelius A, et al. Tumor-specific crosslinking of GITR as costimulation for immunotherapy. J Immunother 2010;33:925–34.
34. Schmiedel BJ, Werner A, Steinbacher J, Nuebling T, Buechele C, Grosse-Hovest L, et al. Generation and preclinical characterization of a Fc-optimized GITR-Ig fusion protein for induction of NK cell reactivity against leukemia. Mol Ther 2013;21:877–86.
35. Pedroza-Gonzalez A, Kwekkeboom J, Sprengers D. T-cell suppression mediated by regulatory T cells infiltrating hepatic tumors can be overcome by GITRL treatment. Oncoimmunology 2013;2:e22450.
36. Schmiedel BJ, Arélin V, Gruenebach F, Krusch M, Schmidt SM, Salih HR. Azacytidine impairs NK cell reactivity while decitabine augments NK cell responsiveness toward stimulation. Int J Cancer 2011;128: 2911–22.
37. Schuijer M, Berns EM. TP53 and ovarian cancer. Hum Mutat 2003;21: 285–91.
38. Pal T, Permuth-Wey J, Betts JA, Krischer JP, Fiorica J, Arango H, et al. BRCA1 and BRCA2 mutations account for a large proportion of ovarian carcinoma cases. Cancer 2005;104:2807–16.
39. Obermajer N, Muthuswamy R, Odunsi K, Edwards RP, Kalinski P. PGE(2)-induced CXCL12 production and CXCR4 expression controls the accumulation of human MDSCs in ovarian cancer environment. Cancer Res 2011;71:7463–70.
40. Triozzi PL, Aldrich W, Achberger S, Ponnazhagan S, Alcazar O, Saunthararajah Y. Differential effects of low-dose decitabine on immune effector and suppressor responses in melanoma-bearing mice. Cancer Immunol Immunother 2012;61:1441–50.
41. Wiltrout RH, Brunda MJ, Holden HT. Variation in selectivity of tumor cell cytolysis by murine macrophages, macrophage-like cell lines and NK cells. Int J Cancer 1982;30:335–42.
42. Weiner LM, Surana R, Wang S. Monoclonal antibodies: versatile platforms for cancer immunotherapy. Nat Rev Immunol 2010;10:317–27.
43. Goyne HE, Cannon MJ. The case for HER2/neu as a therapeutic target for gynecologic malignancies. Immunotherapy 2012;4:781–4.
44. Kost ER, Mutch DG, Herzog TJ. Interferon-gamma and tumor necrosis factor-alpha induce synergistic cytolytic effects in ovarian cancer cell lines-roles of the TR60 and TR80 tumor necrosis factor receptors. Gynecol Oncol 1999;72:392–401.
45. Wang LX, Mei ZY, Zhou JH, Yao YS, Li YH, Xu YH, et al. Low dose decitabine treatment induces CD80 expression in cancer cells and

stimulates tumor specific cytotoxic T lymphocyte responses. PLoS ONE 2013;8:e62924.
46. Li J, Yang Y, Inoue H, Mori M, Akiyoshi T. The expression of costimulatory molecules CD80 and CD86 in human carcinoma cell lines: its regulation by interferon gamma and interleukin-10. Cancer Immunol Immunother 1996;43:213–9.
47. Pechhold K, Patterson NB, Craighead N. Inflammatory cytokines IFN-gamma plus TNF-alpha induce regulated expression of CD80 (B7-1) but not CD86 (B7-2) on murine fibroblasts. J Immunol 1997;58: 4921–9.
48. Vasaturo A, Di Blasio S, Peeters DG, de Koning CC, de Vries JM, Figdor CG, et al. Clinical implications of co-inhibitory molecule expression in the tumor microenvironment for DC vaccination: a game of stop and go. Front Immunol 2013;4:417.
49. Pedicord VA, Montalvo W, Leiner IM, Allison JP. Single dose of anti-CTLA-4 enhances CD8+ T-cell memory formation, function, and maintenance. Proc Natl Acad Sci U S A 2011;108:266–71.
50. Sconocchia G, Eppenberger S, Spagnoli GC, Tornillo L, Droeser R, Caratelli S, et al. NK cells and T cells cooperate during the clinical course of colorectal cancer. Oncoimmunology 2014;3:e952197.